

Teaching Case

Multimodality Imaging Assessment of the Heart Before and After Stage III Non-small Cell Lung Cancer Radiation Therapy



Oi-Wai Chau, BSc,^{a,b,*} Ali Islam, MD,^c Edward Yu, MD,^{a,b} Melody Qu, MD,^b John Butler, MRT,^c Heather Biernaski, MRT,^c Alexander Sun, MD,^d Jean-Pierre Bissonnette, PhD,^d Anna MacDonald, RN,^c Chantelle Graf, RN,^c Aaron So, PhD,^{a,c,e} Gerald Wisenberg, MD,^{c,f} Ting-Yim Lee, PhD,^{a,c,e} Frank S. Prato, PhD,^{a,c} and Stewart Gaede, PhD^{a,b,c}

^aDepartment of Medical Biophysics, Western University, London, Ontario, Canada; ^bDepartment of Physics and Radiation Oncology, London Regional Cancer Program, London, Ontario, Canada; ^cLawson Health Research Institute, London, Ontario, Canada; ^dDepartment of Physics and Radiation Oncology, Princess Margaret Cancer Centre, Toronto, Ontario, Canada; ^eRobarts Research Institute, London, Ontario, Canada; ^fDivision of Cardiology, London Health Sciences Centre, London, Ontario, Canada

Received August 19, 2021; accepted February 7, 2022

Introduction

Radiation may induce unintentional injury of myocardial tissue during and after treatment of non-small cell lung cancer (NSCLC) due to the close proximity of the heart to the target. The Radiation Therapy Oncology Group 0617 clinical trial showed a reduction in median overall survival (OS) for higher radiation doses compared with standard doses in the treatment of NSCLC, with V_{5Gy}Heart being an OS predictor in the first year and median long-term follow-up at the fifth year.¹ Radiation therapy (RT)-related cardiac damage may occur through acute inflammation in both the myocardium and microvasculature and may not be diagnosed until a late stage of the disease. Previously our laboratory demonstrated, in canines imaged with

[¹⁸F] fluorodeoxyglucose (¹⁸FDG)/positron emission tomography (PET), a progressive global inflammatory response during the initial year after RT.² The response was detected as early as 1 week post single fraction irradiation and was confirmed with immunohistochemistry at 12 months.²

Early diagnosis of acute myocardial functional responses to RT has allowed timely and appropriate treatment with cardio-protective drugs such as angiotensin-converting enzyme-inhibitors and/or beta-blockers to reduce the mortality associated with radiation.^{3,4} However, if inflammation occurs early, preceding but predictive of subsequent functional changes, then there may be a role for early treatment with anti-inflammatory and/or cardio-protective medication.

With the use of multimodality imaging, we aimed to assess the effects of RT on inflammatory response, left ventricular function, and myocardial perfusion noninvasively as early as 6 weeks post RT. ¹⁸FDG/PET with glucose suppression of normal myocytes can identify an inflammatory reaction, as the activated proinflammatory macrophages preferentially sequester glucose, for example, cardiac sarcoidosis.⁵ In addition, both functional

Sources of support: This work was supported through a Canadian Institute for Health Research Bridge grant. No conflict of interest, financial or otherwise, are declared by the authors.

Disclosures: none.

Data sharing statement: Research data are stored in an institutional repository and will be shared upon request to the corresponding author.

*Corresponding author: Oi-Wai Chau, BSc; E-mail: ochau@uwo.ca

<https://doi.org/10.1016/j.adro.2022.100927>

2452-1094/© 2022 The Author(s). Published by Elsevier Inc. on behalf of American Society for Radiation Oncology. This is an open access article under the CC BY-NC-ND license (<http://creativecommons.org/licenses/by-nc-nd/4.0/>).

computed tomography (CT) and magnetic resonance imaging (MRI) are often used to quantitatively measure cardiac function to assess cardiac injury after RT. CT perfusion has been shown to have good diagnostic accuracy to identify hemodynamically coronary significant lesions in comparison to the catheter-based fractional flow reserve technique.⁶ Huang et al previously reported mean CT myocardial perfusion reserve (MPR) values in non-ischemic (2.53 ± 0.7) and ischemic segments (1.56 ± 0.41).⁷ The capability of functional MRI to acquire cine images of wall motion throughout the cardiac cycle during short breath holds of 10 to 20 seconds has developed as the gold standard for the quantitation of left ventricular ejection fraction (LVEF), end-systolic, end-diastolic, and stroke volumes (SV).⁸ Marceira et al established reference ranges for healthy men (normal 95% confidence interval of LVEF: 58%-75%; left ventricle end-systolic volume [LVESV]: 30-75 mL; left ventricle end-diastolic volume [LVEDV]: 115-198 mL; and LVSF: 76-132 mL).⁹ The reproducibility of cine MRI in identifying patients with heart failure was also verified.¹⁰

Case Presentations

In this report, 2 NSCLC patient cases are presented. The patients included in this study were recruited under the clinical trial (RICT-Lung: NCT03416972) in 2019 and under the Western University Health Sciences research ethics board approval (109084). Patient 2 of this study was also recruited under the Canadian PET-BOOST clinical trial (NCT02788461)¹¹, which was funded by the Canadian Pulmonary Radiotherapy Investigators Group and under the Ontario Cancer research ethics board approval (1215).

Patient characteristics

Patient 1 (65 years of age) presented with a $4.7 \times 3.2 \times 4.2$ cm moderately differentiated stage III squamous cell carcinoma, T3N2M0,¹² of the left upper lobe, PD-L1 negative (Fig 1). Apart from RT, patient 1 received concurrent chemotherapy with carboplatin and paclitaxel for 6 consecutive weeks followed by 1 year of durvalumab immunotherapy. Patient 1 had a history of coronary artery disease (CAD) with 3 prior myocardial infarctions treated with a total of 5 stents in the left circumflex (LCX) and right coronary (RC) arteries (Fig 2a). Extensive calcified plaque in the left anterior descending artery (LAD) was also identified in the baseline CT image (Fig 2b).

Patient 2 (63 years of age) presented with a $5.2 \times 5.2 \times 8$ cm poorly differentiated adenocarcinoma, T4N2M0, in the left upper lobe with mediastinal invasion. The tumor was EGFR-negative, ALK-negative, and PD-

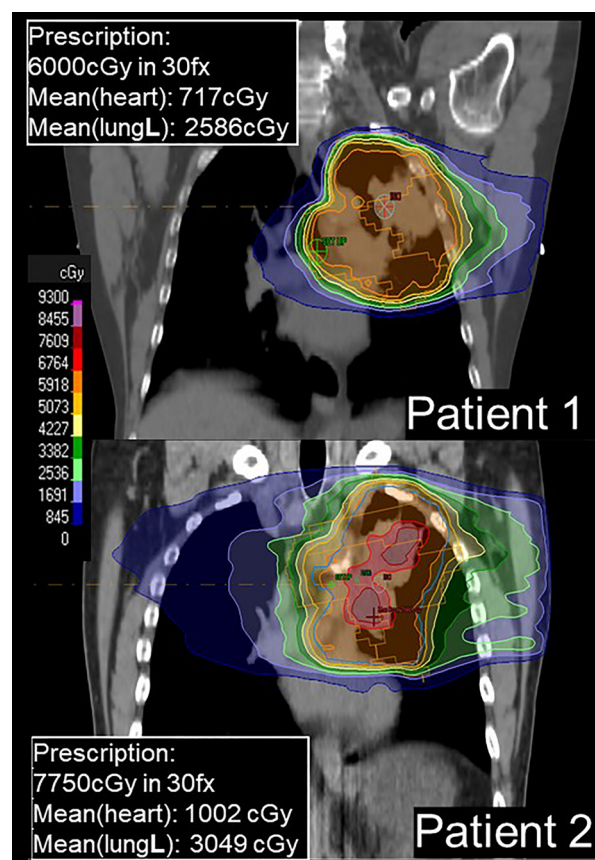


Fig. 1 Dose distribution obtained from the Pinnacle¹³ treatment planning system (Philips Radiation Oncology Systems, Fitchburg) and treatment prescription of each patient, along with their mean heart and left lung doses. Both patients were treated on the 6 MV TrueBeam linear accelerator (Varian Medical Systems, Palo Alto) using volumetric-modulated arc therapy (VMAT). Patient 1 (65 years of age) received standard 60 Gy in 30 fractions. Patient 2 (63 years of age) received 60 Gy in 30 fractions with a simultaneous integrated boost up to 77.5 Gy to the metabolic active tumor subvolume. Note patient 2 received a greater mean heart dose than patient 1.

L1 strongly positive. Patient 2 was treated with concurrent chemotherapy of cisplatin and vinblastine every 21 days for 4 cycles, followed by 1 year of durvalumab immunotherapy.

Treatment planning and delivery

Both patients were treated with 6 MV beams from a medical linear accelerator (TrueBeam Varian Medical Systems, Palo Alto, CA) using volumetric modulated arc therapy. Treatment planning optimization was performed using the Pinnacle¹³ treatment planning system (Philips Radiation Oncology Systems, Fitchburg, MA). Patient 1 was prescribed a standard 60 Gy in 30 fractions to the left

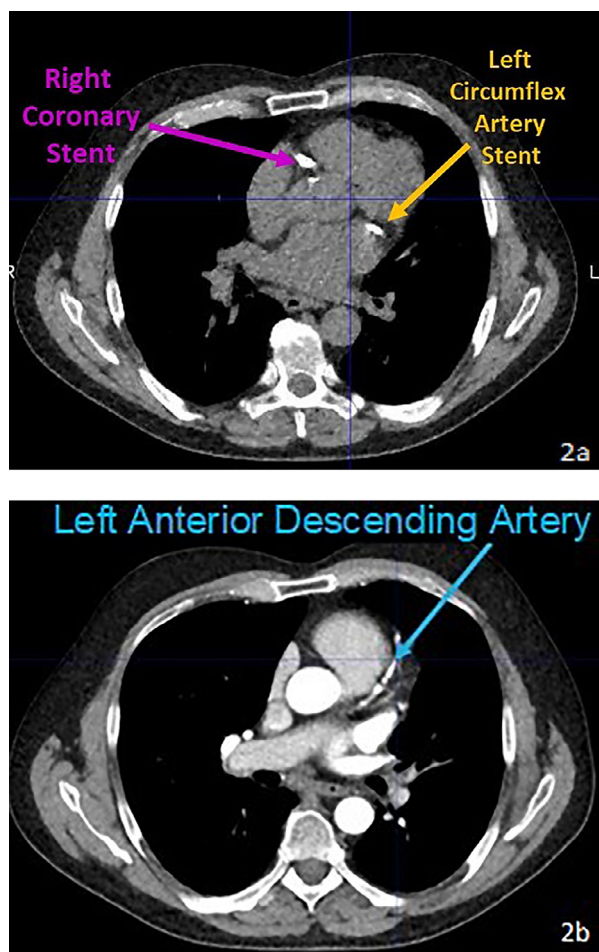


Fig. 2 (a) Patient 1 presented with a history of coronary artery disease including 3 previous myocardial infarctions and intervention with 5 stents. (b) Patient 1 presented with extensive calcified plaque in the left anterior descending artery.

upper tumor. Patient 2 also participated in the clinical trial – Canadian PET-BOOST clinical trial (NCT02788461).¹¹ Here, the planning target volume received a dose of 60 Gy in 30 fractions, while a simultaneous integrated radiation boost of 77.5 Gy was delivered to the metabolic active tumor subvolume. The regions of interest for both patients satisfied the dosimetric guidelines of a standard 60 Gy in 30 fractions NSCLC RT plan in our clinic.

Patient 1 received a mean dose of 7.2 Gy to the heart, 1.1 Gy to the left ventricle (LV), 29.8 Gy to the LAD, 2.0 Gy to the LCX, and 1.0 Gy to the RC artery. Patient 2 received a mean dose of 10.0 Gy to the heart, 4.2 Gy to the LV, 39.8 Gy to the LAD, 2.2 Gy to the LCX, and 1.8 Gy to the RC artery.

In terms of dose distributed in the myocardial segments according to the coronary artery vascular territory, patient 1 received 1.3 Gy to the LCX territory, 0.8 Gy to the LAD territory, and 0.5 Gy to the RC territory, which

was less than patient 2, who received 4.2 Gy to LCX territory, 2.8 Gy to the LAD territory, and 1.3 Gy to the RC artery territory.

Multimodality imaging

Multimodality functional imaging sessions were performed in a single institution at baseline and 6 weeks post RT (see Fig E1 for imaging protocol).

CT perfusion

Initially, an electrocardiogram-gated dynamic contrast-enhanced CT (Iopamidol 370; Bracco Diagnostics, Plainsboro, NJ) was performed on a 256 slice-GE Revolution CT scanner (GE Health care, Waukesha, WI). The scan parameters were the following: 50 cm FOV, 100 kV, 100 mA, 15 passes, minimum 0.8 seconds between passes, 0.28 second rotation time, for a total exposure time of 47.7 seconds. Two free-breathing dynamic scans were obtained including a rest and an adenosine-induced (0.14 $\mu\text{g}/\text{kg}/\text{min}$) stress scan. Middiastolic phase CT images were selected, nonrigidly registered, and averaged into a slice thickness of 2.5 mm. Myocardial perfusion maps were generated with a model-based deconvolution method¹⁴ using the CT Perfusion software (GE Healthcare), with segments delineated according to the approximately horizontal long-axis 6-segment heart model.¹⁵ Absolute myocardial perfusion at rest and post-adenosine was determined as well as MPR.

Myocardial inflammation

The ¹⁸F¹⁸FDG/PET imaging protocol was performed on a 3T-hybrid PET/MR scanner (Biograph mMR; Siemens Medical Systems, Malvern, PA). Both patients fasted for 12 hours before imaging. Intravenous heparin (5 units/kg) was injected initially 45 minutes and then (10 units/kg) 15 minutes before the injection of ¹⁸F¹⁸FDG (5 MBq/kg). PET imaging acquisition was performed in list mode 1 hour after the second injection for 20 minutes, whereas a bellows device was used for respiratory triggering. All PET data were reconstructed using an iterative 3-dimensional (3D) ordered subset expectation maximization algorithm¹⁶ with 3 iterations, 21 subsets, 172 × 172 × 127 matrix size, and a 4-mm Gaussian smoothing filter, yielding a voxel size of 2.08 × 2.08 × 2.03 mm. Attenuation was corrected for all PET scans using a 2-point Dixon MRI pulse sequence. Mean standardized uptake based on body weight of each myocardium segment was analyzed and compared using MIM v7.0.5 (MIM Software Inc, Cleveland, OH).

MRI

The MR 2D stack of standard noncontrast steady state free precession cine imaging of the whole heart was also performed in the same imaging session as PET. The cine images were collected using the TrueFISP sequence

(6 mm slice thickness, 50.82 ms repetition time, 1.58 ms echo time, FOV matrix = 300 × 300). Late gadolinium enhancement (LGE) images were collected using the T1-weighted postcontrast agent (Gadovist; Bayer Inc, Mississauga, ON) Flash3D sequence, 421.09 ms repetition time, 1.2 ms echo time, flip angle 20, and FOV matrix = 270 × 320. T2-weighted images were acquired using TrueFISP 2D sequence with 262.35 ms repetition time, 1.36 ms echo time, and FOV matrix = 300 × 300. Circle CVI42 v5.11 (Circle Cardiovascular Inc, Calgary, Canada) was used to obtain cardiac functional measurements including the LVEDV, LVESV, LVEF, and SV, and for a radiologist (A.I.) to provide clinical assessment of the LGE and T2-weighted images.

Results

Both patients manifested a global increase in the ¹⁸F-DG/PET myocardial uptake at 6 weeks post RT (Table 1 and Fig 3). For CT MPR measurements, different responses were seen between patient 1 who had CAD and patient 2 who did not. Patient 1 had MPR reduction in half of the segments, while patient 2 had a reduction of MPR in all segments (Tables 1 and 2).

For both patients, the LVEF was reduced and LVESV was increased at 6 weeks post RT (Table 3). For patient 1, an increase in LVEDV and SV was observed, while for

patient 2, a reduction in LVEDV and SV was observed at 6 weeks post RT. At follow-up imaging of patient 2, there was a small mid myocardial focus of LGE in the basal inferolateral segment that was not observed at baseline. This corresponded to the region of lowest MPR value. The area of the scar (see Fig E2 for scar with LGE) demonstrated a borderline increase in quantitative T2 relaxation up to 53 ms.

Within 1 year post RT, patient 1 developed increasing cough, shortness of breath after 5 minutes of walking, and hypotension. At 18 months post RT, a slight increase in the size of small pericardial and pleural effusions along with innumerable bilateral pulmonary nodules and new lesions were observed on a follow-up CT thorax image. Based on the evidence of disease progression in the lungs while on durvalumab, patient 1 did not qualify for immunotherapy and passed away at 19 months post RT. For patient 2, no respiratory symptoms, dyspnea on exertion, or chest pain was reported at 1 month follow-up and at every 3 months follow-up to 30 months post RT. No further cardiac functional imaging was performed beyond 6 months for either patient.

Discussion

Currently in the literature, there is no study comparing the cardiac effects before and after NSCLC RT using

Table 1 ¹⁸F-DG/PET mean SUV_{bw} and CT MPR values of the 2 patients are presented

			Left circumflex		Left anterior descending		Right coronary	
			Basal lateral	Mid lateral	Apical lateral	Apical septal	Mid septal	Basal septal
¹⁸ F-DG myocardial mean standard uptake based on body weight mean (SUV _{bw})	Patient 1	Baseline	1.92	1.56	1.02	1.33	1.46	1.63
		Follow-up	3.45	3.28	2.6	3.25	4.11	3.44
		Increase factor	1.8	2.1	2.55	2.44	2.82	2.11
	Patient 2	Baseline	1	0.56	0.21	0.73	1.03	1.21
		Follow-up	1.78	1.52	1.02	1.41	1.92	1.97
		Increase factor	1.78	2.71	4.86	1.93	1.86	1.63
CT myocardial perfusion reserve = stress perfusion/rest perfusion	Patient 1	Baseline	2.42	1.55	1.34	1.58	1.74	2.07
		Follow-up	1.77*	2.28	1.07*	1.65	2.1	1.74*
		Percentage change (%)	−26.9*	47.1	−20.2*	4.4	20.7	−15.9*
	Patient 2	Baseline	2.61	2.27	2.39	2.43	2.78	2.81
		Follow-up	1.37*	1.71*	1.8*	1.66*	1.63*	1.41*
		Percentage change (%)	−47.5*	−24.7*	−24.7*	−31.7*	−41.4*	−49.8*

Abbreviations: CT = computed tomography; ¹⁸F-DG = ¹⁸fluorodeoxyglucose; MPR = myocardial perfusion reserve; PET = positron emission tomography; RT = radiation therapy; SUV_{bw} = standard uptake of the myocardium based on body weight.

* Segments with reduction of MPR at 6 weeks post RT.

The uptake and MPR values were sorted according to the respective supplied coronary arteries using the approximately horizontal long-axis heart model.¹⁵ ¹⁸F-DG/PET increase factor is the calculated ratio of mean ¹⁸F-DG uptake between follow-up and baseline. MPR value is the ratio between adenosine-induced stress perfusion and rest perfusion.

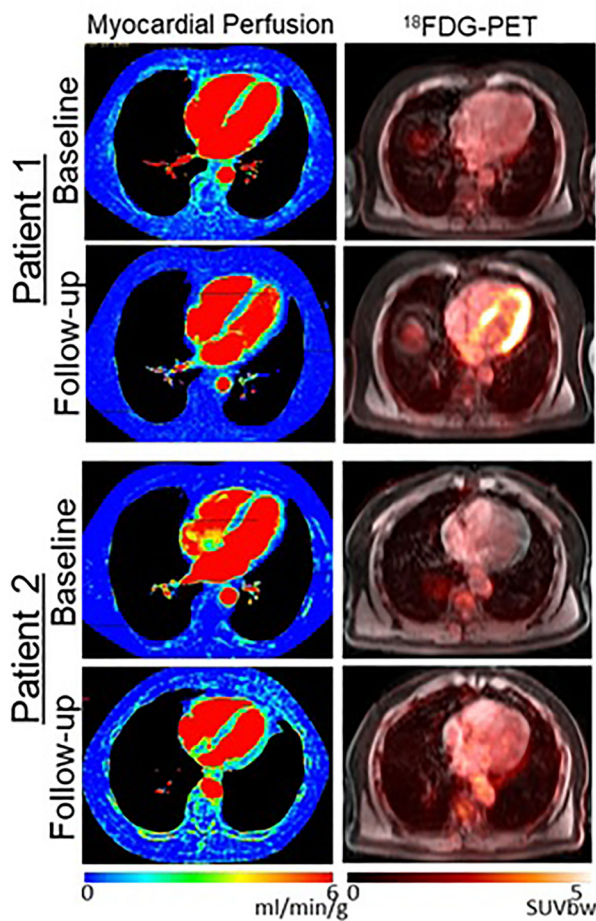


Fig. 3 Baseline and 6-week follow-up of rest computed tomography (CT) myocardial perfusion images and [¹⁸F] fluorodeoxyglucose (¹⁸FDG)/positron emission tomography (PET) images of the heart. Note global increase of myocardial uptake can be seen in post radiation therapy (RT) PET imaging of both patients.

multimodality imaging. Most of the studies that assessed cardiac functional response of RT were performed in breast and Hodgkin lymphoma patients.^{17,18} Demissei et al reported a significant increase in cardiovascular biomarkers in patients after completion of lung cancer RT; however, the changes in biomarkers were not significantly associated with the changes in echocardiography-derived measures of cardiac functional parameters (LVEF, longitudinal circumferential strain).¹⁹ Vinogradskiy et al evaluated ¹⁸FDG/PET imaging changes in terms of the whole heart, with the Kaplan-Meier curves showing an overall trend of improved OS, corresponding with increasing mean standard uptake cardiac values.²⁰ However, the study did not use a protocol for suppression of myocyte glucose uptake, and the time interval between baseline and follow-up imaging (range, 201-1131 days) was inconsistent. Our study is the first to report cardiac functional changes after NSCLC RT using multimodality imaging. Patient 1 CT MPR <2, particularly in the LAD-supplied apical segments at both timepoints, were consistent with the impaired hyperemic response documented in the literature, as indicative of a functionally significant luminal narrowing ≥50% on CT angiography.²¹ Patient 2 baseline MPR values were consistent with no hemodynamically significant attenuation of hyperemia, as reported by Huang et al.⁷ Different responses were observed in MPR in patient 1 compared with patient 2, who did not have CAD. A global reduction of MPR, with the range of 1.37 to 1.8 at follow-up as measured for patient 2, could now be considered to be indicative of an impaired hyperemic response.⁷

In terms of MR functional parameters, both patients had a reduction in LVEF and increase in LVESV; however, different responses were observed in LVESV and SV in patient 1 compared with patient 2, who did not have CAD. At both imaging timepoints, the MR functional

Table 2 CT myocardial perfusion values under rest and adenosine-induced stress scans of the 2 patients are presented

	CT perfusion (mL/min/100g)	Left circumflex		Left anterior descending			Right coronary
		Basal lateral	Mid lateral	Apical lateral	Apical septal	Mid septal	Basal septal
Patient 1 baseline	Rest	344.72	351.17	605.13	576.93	423.24	471.08
	Stress	834.22	544.32	810.87	911.55	736.44	975.14
Patient 1 follow-up	Rest	142.50	125.72	182.63	178.18	142.69	166.88
	Stress	251.62	287.18	195.04	294.15	298.99	290.67
Patient 2 baseline	Rest	56.02	70.48	81.30	92.51	67.61	60.29
	Stress	146.14	159.67	194.25	224.83	187.89	169.55
Patient 2 follow-up	Rest	119.90	113.14	121.29	161.95	122.03	129.24
	Stress	164.81	193.17	218.86	268.40	198.36	182.18

Abbreviation: CT = computed tomography.

The perfusion values are sorted according to the respective supplying coronary arteries using the approximately horizontal long-axis heart model.¹⁵

Table 3 Presented are cardiac functional parameters including the LVESV, LVEDV, SV, and the LVEF for the 2 patients before and after radiation therapy

		LVESV (mL)	LVEDV (mL)	SV (mL)	LVEF (%)
Patient 1	Baseline	49	138	89	65
	Follow-up	55	151	96	64*
	Percentage change (%)	11.5	9.2	8	−1.5*
Patient 2	Baseline	64	166	102	61
	Follow-up	75	164*	89*	54*
	Percentage change (%)	16.7	−1.4*	−12.8*	−11.4*

Abbreviations: LVEDV = left ventricle end-diastolic volume; LVEF = left ventricle ejection fraction; LVESV = left ventricle end-systolic volume; RT = radiation therapy; SV = stroke volume.

* Functional indicators with reduction at 6 weeks post RT.

measurements reported for patient 1 were within the normal range, whereas for patient 2 at follow-up, the LVEF was slightly under the normal range by 4%.⁹ The LGE of myocardial focus in patient 2 at follow-up may be consistent with local edema suggestive of acute inflammation in the cardiac region, which received the highest radiation dose. From the ¹⁸FDG/PET results, the elevated global myocardial uptake suggested an acute inflammation response to RT for both patients.

It is unlikely that such a complex set of tests used here would be routinely used for patient management. Current routine tests typically include echocardiography and blood work. As a scar would be expected to develop only subsequent to inflammation, the ¹⁸FDG/PET signal suggesting inflammation may be more sensitive to a pathologic response to RT than MR, which is looking for scar development. However, the additional step of suppression of myocardial uptake of ¹⁸FDG is required for optimal ¹⁸FDG/PET test results. The assessment of MPR with any modality (performed here with CT) requires the use of a pharmacologic stressor such as adenosine, which was used in this study.

Our pilot study with 2 patients with NSCLC representing 2 different baseline cardiac conditions demonstrated the feasibility of using multimodality imaging in detecting early functional changes of the heart. The presence of these changes might indicate a risk for late manifestations and may be a focus of future therapeutic interventions to improve radiation-mediated outcomes. Therefore, further long-term follow-up studies in a larger cohort need to confirm the functional responses (¹⁸FDG/PET, MPR, and LV function) as accurate predictors of radiation-induced clinically important cardiac toxicity before the routine use of these expensive imaging modalities. If validated, we expect mitigation strategies could be applied and/or developed to protect the heart from radiation toxicity at an early timepoint.

Conclusions

In summary, these 2 cases demonstrate the feasibility of using multimodality imaging to assess cardiac responses to radiation therapy as early as 6 weeks after the end of radiation therapy. Quantitative assessment included CT perfusion, ¹⁸FDG/PET measured inflammation uptake, and MR cardiac functional metrics before and after radiation therapy (6 weeks) that were obtained from 2 dynamic imaging sessions. Both patients with NSCLC experienced a global increase in ¹⁸FDG/PET myocardium uptake, increase in LVESV, and decrease in LVEF, while CT MPR and MR functional measurements suggested a different response in the patient with a history of CAD (regional ranges of CT MPR and increase of LVEDV and SV) compared with the patient with no history of CAD (global MPR, LVEDV, and SV reduction). Validation of these results in additional patients with and without CAD can advance decision making for NSCLC treatment.

Acknowledgments

The authors would like to acknowledge the participating clinical trial patients and members of their families, as well as Dr William Pavlosky, Tony Wales, and Jennifer Hadway (St. Joseph's Hospital, London, ON, Canada) for technical support on the project.

Supplementary materials

Supplementary material associated with this article can be found in the online version at [doi:10.1016/j.adro.2022.100927](https://doi.org/10.1016/j.adro.2022.100927).

References

- Bradley J, Hu C, Komaki R, et al. Long-term results of NRG Oncology RTOG 0617: Standard versus high-dose chemoradiotherapy with or without cetuximab for unresectable stage III non-small-cell lung cancer. *J Clin Oncol*. 2020;38:706–714.
- El-Sherif O, Xhaferllari I, Sykes J, et al. [¹⁸F]FDG cardiac PET imaging in a canine model of radiation-induced cardiovascular disease associated with breast cancer radiotherapy. *Am J Physiol Heart Circ Physiol*. 2019;316:H586–595.
- Ohtsuka T, Hamada M, Hiasa G, et al. Effect of beta-blockers on circulating levels of inflammatory and anti-inflammatory cytokines in patients with dilated cardiomyopathy. *J Am Coll Cardiol*. 2001;37:412–417.
- Kortekaas K, Meijer A, Hinnen JW, et al. ACE inhibitors potently reduce vascular inflammation, results of an open proof-of-concept study in the abdominal aortic aneurysm. *PLoS One*. 2014;9:e111952.
- Wisenberg G, Thiessen J, Pavlosky W, et al. Same day comparison of PET/CT and PET/MR in patients with cardiac sarcoidosis. *J Nucl Cardiol*. 2020;27:2118–2129.
- Bamberg F, Becker A, Schwarz F, et al. Detection of hemodynamically significant coronary artery stenosis: Incremental diagnostic value of dynamic CT-based myocardial perfusion imaging. *Radiology*. 2011;260:689–698.
- Huang L, Wu MT, Hu C, et al. Quantitative low-dose rest and stress CT myocardial perfusion imaging with a whole-heart coverage scanner improves functional assessment of coronary artery disease. *Int J Cardiol Heart Vasc*. 2019;24: 100381.
- Grothues F, Smith G, Moon J, et al. Comparison of interstudy reproducibility of cardiovascular magnetic resonance with two-dimensional echocardiography in normal subjects and in patients with heart failure or left ventricular hypertrophy. *Am J Cardio*. 2002;90:29–34.
- Maceira A, Prasad S, Pennell D. Normalized left ventricular systolic and diastolic function by steady state free precession cardiovascular magnetic resonance. *J Cardiovasc Magn Reson*. 2006;8:417–426.
- Bellenger N, Davies L, Francis J, Coats A, Pennell D. Reduction in sample size for studies of remodelling in heart failure by the use of cardiovascular magnetic resonance. *J Cardiovasc Magn Reson*. 2000;2:271–278.
- Raman S, Bissonnette J-P, Warner A, et al. Rationale and protocol for a Canadian multicenter Phase II randomized trial assessing selective metabolically adaptive radiation dose escalation in locally advanced non-small-cell lung cancer (NCT02788461). *Clin Lung Cancer*. 2018;19:e699–703.
- Frank D. The eight edition TNM stage classification for lung cancer: What does it mean on main street? *J Thoracic Cardiovasc Surg*. 2018;155:356–359.
- Cadman P, McNutt T, Bzdusek K. Validation of physics improvements for IMRT with a commercial treatment-planning system. *J Appl Clin Med Phys*. 2005;6:74–86.
- So A, Hsieh J, Li JY, Hadway J, Kong HF, Lee TY. Quantitative myocardial perfusion measurement using CT perfusion: A validation study in a porcine model of reperfused acute myocardial infarction. *Int J Cardiovasc Imaging*. 2012;28:1237–1248.
- Cerqueria M, Wesissman N, Dilsizian V, et al. Standardized myocardial segmentation and nomenclature for tomographic imaging of the heart. *Circulation*. 2002;105:539–542.
- Hudson H, Larkin R. Accelerated image reconstruction using ordered subsets of projection data. *Med Imaging IEEE Trans*. 1994;13:601–609.
- Kaidar-Person O, Zagar T, Oldan J, et al. Early cardiac perfusion defects after left-sided radiation therapy for breast cancer: Is there a volume response? *Breast Cancer Res Treat*. 2017;164:253–262.
- Heckmann M, Totakhel B, Finke D, et al. Evidence for a cardiac metabolic switch in patients with Hodgkin's lymphoma. *ESC Heart Failure*. 2019;6:824–829.
- Demissei B, Freedman G, Feigenberg S, et al. Early changes in cardiovascular biomarkers with contemporary thoracic radiation therapy for breast cancer, lung cancer, and lymphoma. *Int J Radiat Oncol Biol Phys*. 2019;103:851–860.
- Vinogradskiy Y, Diot Q, Jones B, et al. Evaluating positron emission tomography-based functional imaging changes in the heart after chemo-radiation for patients with lung cancer. *Int J Radiat Oncol Biol Phys*. 2020;106:1063–1070.
- Fiechter M, Ghadri J, Gebhard C, et al. Diagnostic value of ¹³N-ammonia myocardial perfusion PET: Added value of myocardial flow reserve. *J Nucl Med*. 2012;53:1230–1234.